THE JOURNAL OF BIOLOGICAL CHEMISTRY VOL. 287, NO. 31, pp. 26155–26166, July 27, 2012

The DEAD-box RNA Helicase Dbp2 Connects RNA Quality Control with Repression of Aberrant Transcription*◆

Received for publication, May 17, 2012, and in revised form, June 6, 2012 Published, JBC Papers in Press, June 7, 2012, DOI 10.1074/jbc.M112.383075

Sara C. Cloutier, Wai Kit Ma, Luyen T. Nguyen, and Elizabeth J. Tran[1]

From the Department of Biochemistry and Purdue Cancer Center, Purdue University, West Lafayette, Indiana 47907-2063

Background: Dbp2 is a member of the DEAD-box family of RNA helicases.
Results: Dbp2 is a double-stranded RNA-specific ATPase required for repression of cryptic initiation and downstream RNA quality control.
Conclusion: Dbp2 functions in transcriptional fidelity as a cotranscriptional RNA chaperone.
Significance: Elucidation of key RNA enzymes is central to defining the mechanisms for eukaryotic gene regulation.

DEAD-box proteins are a class of RNA-dependent ATP hydrolysis enzymes that rearrange RNA and RNA-protein (ribonucleoprotein) complexes. In an effort to characterize the cellular function of individual DEAD-box proteins, our laboratory has uncovered a previously unrecognized link between the DEAD-box protein Dbp2 and the regulation of transcription in *Saccharomyces cerevisiae*. Here, we report that Dbp2 is a double-stranded RNA-specific ATPase that associates directly with chromatin and is required for transcriptional fidelity. In fact, loss of *DBP2* results in multiple gene expression defects, including accumulation of noncoding transcripts, inefficient 3′ end formation, and appearance of aberrant transcriptional initiation products. We also show that loss of *DBP2* is synthetic lethal with deletion of the nuclear RNA decay factor, *RRP6*, pointing to a global role for Dbp2 in prevention of aberrant transcriptional products. Taken together, we present a model whereby Dbp2 functions to cotranscriptionally modulate RNA structure, a process that facilitates ribonucleoprotein assembly and clearance of transcripts from genomic loci. These studies suggest that Dbp2 is a missing link in RNA quality control that functions to maintain the fidelity of transcriptional processes.

Essential cellular processes, such as growth, organ development, and differentiation, require precise spatial and temporal control of gene expression. Eukaryotic gene expression involves highly complex and coordinated events, including transcription, pre-messenger RNA (pre-mRNA) processing, mRNA transport to the cytoplasm, translation, and decay. During synthesis, RNA-binding proteins and complexes dynamically associate with the RNA to form a mature, translationally competent mRNP[2] complex (1). These factors promote proper pre-mRNA processing and transport as well as couple upstream and downstream steps in the gene expression network. In addition to protein-coding mRNAs, the eukaryotic genome also encodes numerous noncoding RNAs (2–4). These include well known members such as transfer RNAs, ribosomal RNAs, and spliceosomal RNAs, as well as a more recently recognized class of heterogeneous long noncoding RNAs (lncRNAs) (5). The latter class has recently gained importance due to the conserved nature of this widespread transcription and connections between specific members and epigenetic gene regulatory mechanisms (6).

In the budding yeast *Saccharomyces cerevisiae*, lncRNAs are very low in abundance and have been classically defined based on the inhibited RNA-decay mechanism used for detection. This has resulted in numerous names such as cryptic unstable transcripts, stable untranslated transcripts, and Xrn1-dependent transcripts (5). Whereas the precise function of these molecules is still hotly debated, it is clear that regulation is accomplished through the same mechanisms as those utilized for protein-coding mRNAs. In fact, lncRNAs are substrates for the nuclear exosome, a multiprotein complex responsible for maturation and degradation of numerous noncoding RNAs and aberrantly processed mRNAs (7). This suggests that the signature of a noncoding or aberrant mRNA lies within the targeted RNA molecule itself. Consistent with this, numerous studies have underscored the importance of RNP composition as failure to properly assemble mRNPs results in selective retention and subsequent nuclear degradation (7–10). However, the molecular basis for discrimination of aberrant *versus* mature mRNPs is not fully understood.

One class of enzymes that functions as critical regulators of RNP assembly are the DEAD-box RNA helicases. DEAD-box proteins are RNA-dependent ATPases that function in all aspects of RNA biology, including transcription, mRNA export, and ribosome biogenesis. DEAD-box proteins are the largest group within the RNA helicase superfamily with ~25 members in the budding yeast *S. cerevisiae* and ~40 in humans (11). Numerous studies have shown that DEAD-box proteins display a wide variety of biochemical activities *in vitro*, which includes RNA duplex unwinding, RNA folding, and RNP remodeling (12–14). In contrast to *in vitro* analyses, however, little is known regarding the precise biological function of individual DEAD-box protein family members.

* This work was supported, in whole or in part, by National Institutes of Health Grant R01GM097332 (to E. J. T.).
◆ This article was selected as a Paper of the Week.
[1] To whom correspondence should be addressed: Dept. of Biochemistry, Purdue University, BCHM 305, 175 S. University St., West Lafayette, IN. Tel.: 765-496-3889; Fax: 765-494-7897; E-mail: ejtran@purdue.edu.
[2] The abbreviations used are: mRNP, messenger ribonucleoprotein complex; RNP, ribonucleoprotein; dsRNA, double-stranded RNA; 6AU, 6-azauracil; RT-qPCR, reverse transcriptase-quantitative PCR; lncRNA, long noncoding RNA; 5′RACE, 5′-rapid amplification of cDNA ends.

TABLE 1
Yeast and bacterial plasmids

Name	Description	Source/Ref.
pUG6	KanMx disruption cassette plasmid	23
BTP13	pET28a-*DBP2*	This study
BTP18	pET28a-*dbp2-E268Q*	This study
BTP21	pET28a-*dbp2-K136N*	This study
pDBP2	*DBP2*-PL-ADH-P415	19
BTP24	*pdbp2-K136N/CEN/LEU2*	This study
BTP25	*pdbp2-E268Q/CEN/LEU2*	This study
pCEN/URA3	pRS316	24
pCEN/LEU2	pRS315	24
p3×FLAG	p3 × FLAG:KanMx	25
pGAL1-GAL10-GAL7	pYGPM11l14	Open Biosystems (Genomic Tiling)
pFLO8	pGAL-YER109C	Open Biosystems (Yeast ORF Collection)
pSCR1	YGPM29b01	Open Biosystems (Genomic Tiling)

TABLE 2
Yeast strains

Strain	Genotype	Source
Wild type (BY4741)	MATa *his3Δ1 leu2Δ0 met15Δ0 ura3Δ0*	Open Biosystems
DBP2-GFP	MATa *DBP2-GFP:HIS3 his3D1 leu2D0 met15D0 ura3D0*	Invitrogen
xrn1Δ	MATa *xrn1::KanMx his3D1 leu2D0 met15D0 ura3D0*	Open Biosystems
dbp2Δ (BTY115)	MATa *dbp2::KanMx ura3Δ0 leu2Δ0 his3Δ0 TRP1 met- lys?*	This study
dbp2-K136N (BTY166)	MATa *dbp2::KanMx ura3Δ0 leu2Δ0 his3Δ0 TRP1 met- lys? + pdbp2-K136N/CEN/LEU2*	This study
dbp2-E268Q (BTY180)	MATa *dbp2::KanMx ura3Δ0 leu2Δ0 his3Δ0 TRP1 met- lys? pdbp2-E268Q/CEN/LEU2*	This study
Wild type (FY120)	MATa *his4-912∂ lys2-128∂ leu2Δ1 ura3-52*	26
prGAL-FLO8:HIS3 (FY2393)	MATa *lys2-128∂ his3Δ200 ura3-52 leu2Δ1 trp1Δ63 prGAL1-FLO8-HIS3:KanR*	27
spt6-1004 (FY2139)	*MATα FLAG-spt6-1004 ura3-52 leu2Δ1 lys2-128∂*	27
spt6-1004 prGAL-FLO8:HIS3 (BTY217)	MAT*α spt6-1004-FLAG prGAL-FLO8-HIS3::KanMx ura3-52 leu2Δ1 lys2-128∂ his4-912∂ trp?*	Reconstructed from Ref. 28
dbp2Δ prGAL-FLO8:HIS3 (BTY124)	MAT*α dbp2::KanR prGAL1-FLO8-HIS3::KanMx ura3 leu2 his3 trp? lys? met?*	This study
rrp6Δ	MATa *rrp6::KanMx his3D1 leu2D0 met15D0 ura3D0*	Open Biosystems
DBP2-3×FLAG (BTY200)	MATa *DBP2-3×FLAG:KanMx his3Δ1 leu2Δ0 met15Δ0 ura3Δ0*	This study
Wild type *FT4* (JOU538)	*MATa ura3-52 trp1-Δ63 his3-Δ200 leu2::PET56*	29
FT4 + Reb1BSΔ (JOU811)	*MATa ura3-52 trp1-Δ63 his3-Δ200 leu2::PET56 gal10::URA3::pMV12* (*EcoRI/XhoI-Reb1 BSΔ with BS2 silent*)	29
dbp2Δ FT4 (BTY219)	*MATa ura3-52 trp1-Δ63 his3-Δ200 leu2::PET56 dbp2::KanMx*	This study
dbp2Δ FT4+Reb1BSΔ (BTY220)	*MATa ura3-52 trp1-Δ63 his3-Δ200 leu2::PET56 gal10::URA3::pMV12* (*EcoRI/XhoI-Reb1 BSΔ with BS2 silent*) *dbp2::KanMx*	This study

One largely uncharacterized DEAD-box protein in *S. cerevisiae* is Dbp2. In mammalian cells, the ortholog of Dbp2, termed p68, functions in ribosome biogenesis as well as numerous transcriptional and cotranscriptional processes with RNA polymerase II (15). Dbp2, however, has only been linked to ribosome biogenesis and non-sense-mediated decay in *S. cerevisiae* despite the fact that human p68 functionally complements loss of *DBP2* (16–18). This suggests that a role in transcriptional processes is either not conserved or that Dbp2 plays an as-of-yet uncharacterized function in budding yeast.

In this study, we undertook a directed approach to define the role of Dbp2 in budding yeast. Our studies now provide documentation that Dbp2 functions at the interface of chromatin and RNA structure to represses expression of aberrant transcripts. We suggest that Dbp2 is a missing link in the gene expression network that functions as a cotranscriptional RNA chaperone. This would provide a model RNA modulation during transcription with broad implications to other aspects of RNA biology.

EXPERIMENTAL PROCEDURES

Plasmids and Cloning—All plasmids were constructed by standard molecular biology techniques and are listed in Table 1. *DBP2* was expressed in yeast using the intronless p*DBP2*-PL-ADH-p415 (19) to avoid splicing-dependent changes in expression levels. ATPase-deficient variants were constructed by site-directed mutagenesis using *Pfu* polymerase. The pET28a-*DBP2* was generated by subcloning techniques from p*DBP2*-PL-ADH-p415.

Yeast Manipulations—Yeast strains were constructed using classical yeast genetic techniques and are listed in Table 2. *DBP2*-deletion strains (*dbp2Δ*) were constructed by PCR-based gene replacement using pUG6 as a template. *DBP2–3×FLAG* strains were constructed similarly using the p3×FLAG plasmid. 6AU studies were conducted with yeast strains grown in synthetic media −uracil (−URA) + 2% glucose and spotted onto −URA plates with or without 100 μg/ml 6-azauracil (Sigma). For all RNA analyses, yeast strains were grown in rich YPD media (YP + 2% glucose) at either 35 or 30 °C as indicated to an OD of 0.4–0.5 prior to cell harvesting and RNA isolation. Transcriptional induction was performed by shifting yeast cells from YPD to YP + 1% raffinose for 1 h, to induce a derepressed state, and then to YP-Gal (YP + 2% galactose) for 5 h prior to cell harvesting.

Recombinant Protein Purification—Expression of pET28a HIS_6-*DBP2* in Rosetta *Escherichia coli* (DE3) cells (Novagen) was induced by 0.2 mM isopropyl 1-thio-β-D-galactopyranoside overnight at 16 °C. Cells were lysed in 20 mM Tris at pH 7.9, 100 mM NaCl, 5 mM imidazole. Recombinant proteins were purified from the soluble fraction using nickel affinity chromatography according to the manufacturer's instructions (Qiagen).

In Vitro ATPase Assays—*In vitro* ATP hydrolysis assays were performed using a PK/lactate dehydrogenase enzyme-coupled absorbance assay as described previously (20) but with 440 nM

Dbp2 and total yeast RNA (Sigma) or purchased DNA or RNA oligonucleotides (IDT). k_{obs} values were calculated using the following formula: $V_0 = (A_{340}/\text{min} \times 2.5)/(6.22 \times 10^{-3}\ \mu\text{M})$, where $k_{obs}(\text{min}^{-1}) = V_0/\text{protein concentration}$, and the EC_{50} was determined using GraphPad Prism software. V_0 was normalized to background NADH loss in buffer alone for each condition. Presented data are the average of three independent experiments.

Cellular Microscopy—Wild type (BY4741) or *DBP2-GFP* strains were grown at 30 °C in YPD and were subsequently fixed with 10% formaldehyde, washed with PBS, and stained with 2 μg/ml DAPI (Sigma) for visualization of DNA. Images were collected using an Olympus BX51 fluorescent microscope and Metamorph TL software (Olympus America).

RT-qPCR and 5′RACE—RNA was isolated from cells by standard acid phenol purification. Complementary DNA (cDNA) was prepared using the Quantitect reverse transcriptase kit (Qiagen) according to manufacturer's instructions using random hexamer primers provided. Primer pairs for qPCR were designed using default parameters in Primer Express 3.0 (Invitrogen) and are listed in Table 3. PCRs were performed in the Bio-Rad CFX96 system. Fold changes were calculated using the Pfaffl method (22) and are reported as three biological replicates with three technical repeats each with mean ± S.E. 5′RACE of *GAL7* mRNA was conducted according to the manufacturer's protocol (Invitrogen). *GAL7* gene-specific primers (GSP primers) are listed in Table 4. Resulting 5′RACE products were cloned using a UA cloning kit (Qiagen), and precise 5′ ends were determined by DNA sequencing.

Chromatin Immunoprecipitation—Chromatin immunoprecipitation experiments were conducted as described previously (21) with the following changes. Input represents 2.5% of lysate. Anti-FLAG antibodies (M2, Sigma) were preincubated with protein G Dynabeads (Invitrogen) prior to incubation with cross-linked sheared lysate. Immunoprecipitated DNA was eluted with 400 μl of elution buffer (1% SDS, 0.1 M $NaHCO_3$) followed by reversal of cross-links by addition 16 μl of 5 M NaCl and a 65 °C overnight incubation. Resulting DNA was incubated with RNase A and proteinase K, phenol-extracted, and ethanol-precipitated. Samples were resuspended in 50 μl of TE, and 1:50 was used for qPCR using PrimeTime assay probes listed in Table 5 (IDT) and TaqMan qPCR mix (Invitrogen). All ChIP experiments were conducted with three biological replicates with four technical repeats and are shown as the fold increase above wild type signal relative to input.

Northern Blotting—20–50 μg of total RNA was resolved on a 1.2% formaldehyde-agarose gel followed by transfer to a nylon membrane (Brightstar Hybond N^+, Invitrogen). Northern blotting was conducted using standard methods. Radiolabeled double-stranded DNA probes were generated using PCR products from a plasmid template (see Table 6) and the Decaprime II kit according to manufacturer's instructions (Invitrogen). Transcripts were visualized using a PhosphorImager (GE Healthcare) and quantified by densitometry (ImageQuant, GE Healthcare).

TABLE 3
RT-qPCR oligonucleotides
F is forward and R is reverse.

1 F	TGAGTTCAATTCTAGCGCAAAGG
1 R	TTCTTAATTATGCTCGGGCACTT
2 F	GAGGTCTTGACCAAGCATCACA
2 R	TTCCAGACCTTTTCGGTCACA
3 F	AAATGAAGGTTTGTGTCGTGA
3 R	AAGCTTTGCAGAATGCATGA
4 F	TGAACAAGCCATATGGAGACA
4 R	CGACGATATTACCCGTAGGAA
5 F	CAAAAAGCGCTCGGACAACT
5 R	GCTTGGCTATTTTGTGAACACTGT
6 F (or GAL7 F)	CAAAAAGCGCTCGGACAACT
6R (or GAL7 R)	GCTTGGCTATTTTGTGAACACTGT
7 F	TCAACAGGAGGCTGCTTACAAG
7 R	CCAGGACATAGATAGCATTTTGGA
8 F	CCATTCCACAAATGAAACAATC
8 R	ACAACCCATGGCTGTACCTT
CLB2 F	GCGAATAATCCAGCCCTAAC
CLB2 R	CGGCTGTTGATCTTGATACG
POL1 F	CAGAAAGCGCCAGGAATTG
POL1 R	CGTAGCCTACACCATCGTCATC
RAD 14 F	CCGGCCTCTCGCAGTTACTA
RAD14 R	GCGGCTGCTGCATTATCAT
ACT1 F	TGGATTCCGGTGATGGTGTT
ACT1 R	TCAAAATGGCGTGAGGTAGAGA
ADE3 F	CCCGTGATATCGCATCATACTTAC
ADE3 R	GGCCGATGGCAACGACTA

TABLE 4
5′RACE primers

GAL7-GSP1	GTCCTCCTTCACCATTTGG
GAL7-GSP2	GGCCCAGTATGGAACAACAAC
GAL7-GSP3	CGTCAGTCAATGCTTGCCAAG

RESULTS

DBP2 Is an RNA-dependent ATPase in Vitro—Dbp2 is a member of the DEAD-box family of RNA-dependent ATPases in *S. cerevisiae* based on the presence of 10 conserved sequence motifs organized into two distinct structural domains (Fig. 1*A*) (11). Dbp2 also contains a C-terminal RGG motif and a unique N terminus implicated in high affinity RNA and protein binding *in vivo*, respectively (18, 33).

Although studies from other laboratories have utilized genetic manipulations to assess the enzymatic function of Dbp2 *in vivo* (16, 18, 33), Dbp2 has not been biochemically character-

TABLE 5
Oligonucleotides for chromatin immunoprecipitation

Name	Forward	Reverse	Probe	Relative to +1 Start	+1 Start Refs.
GAL7 P	GCGCTCGGACAACTGTTG	TTTCCGACCTGCTTTTATATCTTTG	CCGTGATCCGAAGGACTGGCTATACA	−66	30
GAL7 5′	ATCATACAATGGAGCTGTGGG	CTAGCCATTCCCATAGACGTTAC	AAGCAGCCTCCTGTTGACCTAACC	+190	30
GAL7 middle	TGCGAAACTTCACTAGGGATG	CCAGAGAAGCAAAGAAAATCATAAG	CAACCCATGGCTGTACCTTTGTTTTCA	+587	30
GAL7 3′	GCATTTCTACCCACCTTTACTGAG	CAGCTTGTTCCGAAGTTAAATCTC	AGGCTCACCTAACAATTCAAAACCAACC	+1079	30
GAL7 3′ UTR	GGACCACTCTTACATAACTAGAATAGC	TTTTCTATTAACTGCCTGGTTTCTTT	TGTCACTCCGTTCAAGTCGACAACC	+1259	30, 31
POL1 5′	AGAATACAGGGCCAGAAAGC	GTAGCCTACACCATCGTCATC	ACAACAAATCGTCATGCAGCAATTCCT	+125	31
RAD14 5′	TGTGTTTGTATTTTAACCGTGGG	GATTCAATTGGTCGCTACTCAG	TGTTAGCCTCCTGCACAGCTCATC	+211	31
CLB2 5′	TCCAGCCCTAACAAATTTCAAATC	GCTGTTGATCTTGATACGCTTTC	TCCGACTTCCCTCCTTCTTTACTGAGTT	+1634	32
ADE3 5′	TGGCTGGTCAAGTGTTGG	TGGTCTGTTGCCTACTTGAATG	TCAAAAGCATTCAAGGTCACGTGCC	+100	31

TABLE 6
Oligonucleotides for Northern blotting (dsDNA probes)
F is forward, and R is reverse.

FLO8 F	CTGTATCCAGTCCATTATCTTCAG
FLO8 R	TCAGCCTTCCCAATTAATAAAATTG
SCR1 F	GGATACGTTGAGAATTCTGGCCGAGG
SCR1 R	AATGTGCGAGTAAATCCTGATGGCACC
GAL7 F	CCTTGGTTAGGTCAACAGGAG
GAL7 R	AGTCGCATTCAAAGGAGCC

ized to date. To determine whether Dbp2 is a functional RNA-dependent ATPase, we established *in vitro* ATPase assays with recombinant purified Dbp2 and increasing amounts of total RNA as described previously (20). Consistent with other DEAD-box enzymes, our results demonstrate that Dbp2 is an active ATPase *in vitro* with a 50% effective concentration (EC_{50}) of 27 μg/ml for RNA (Fig. 1*B*). Next, we used site-directed mutagenesis to incorporate amino acid substitutions in motif I or II and assayed ATP hydrolysis of the resulting purified proteins to verify the origin of wild type Dbp2 activity (Fig. 1*A*). This revealed that both the K136N (motif I) and E268Q (motif II) substitutions abolish enzymatic activity at RNA concentrations 1- and 3-fold above the EC_{50}, consistent with mutations of other DEAD-box enzymes (Fig. 1*C*). Thus, Dbp2 is a functional RNA-dependent ATPase *in vitro*.

To determine whether the enzymatic activity of Dbp2 is required for normal cell growth, we utilized a plasmid complementation assay (Fig. 1*D*). To this end, we generated a *dbp2*Δ strain and analyzed the ability of wild type or ATPase-deficient *dbp2* alleles, p*dbp2-K136N* and p*dbp2-E268Q*, to confer cell growth as compared with vector alone. Consistent with previous reports, loss of *DBP2* results in slow growth and cold sensitivity with an optimal growing temperature of 35 °C (18, 19, 33). Importantly, neither point mutant restored wild type growth, paralleling the growth of the *dbp2*Δ strain with vector alone (Fig. 1*D*). This is in contrast to ectopic expression of the wild type *DBP2* (*pDBP2*), which enabled growth at all temperatures. Immunoblotting analysis verified that the inability of the mutant plasmids to rescue the *dbp2*Δ strain is not due to expression differences between the wild type (p*DBP2*) and mutant *dbp2* vectors (data not shown). Thus, substitutions that impair enzymatic activity also impair cell growth, underscoring a requirement for enzymatically active Dbp2 in budding yeast.

Dbp2 Is a dsRNA-directed ATPase—Given that the ATPase activity of Dbp2 is required for growth, we next asked if Dbp2 preferred specific RNAs for stimulation of ATP hydrolysis. This would indicate a preference for specific RNAs *in vivo*. To test this, we conducted *in vitro* ATPase assays as above in the presence of single-stranded RNA molecules of different lengths (16- or 37-mer) or dsRNA with a GNRA tetraloop ($\Delta G = -25$ kcal/mol; Fig. 2*A*). Strikingly, this revealed that Dbp2 strongly prefers dsRNA for activation of ATP hydrolysis with a resulting EC_{50} of $10^{-6.5}$ or ~0.3 μM (Fig. 2*B*). This is near the concentration of Dbp2 (0.2 μM), suggesting that the affinity is likely higher with the EC_{50} representing the upper limit of the dissociation constant. Strikingly, a longer 37-mer single-stranded RNA is also able to stimulate RNA-dependent ATPase activity but to a significantly lower extent that impairs affinity measurement. This was in contrast to the shorter 16-nucleotide single-stranded RNA, which was unable to activate Dbp2 at any concentration. Importantly, Dbp2 displayed no DNA-directed ATPase activity (Fig. 2*C*). This suggests that Dbp2 displays dsRNA-dependent ATPase activity, an enzymatic parameter that parallels human p68 but is not common among other DEAD-box family members (34, 35). Furthermore, preliminary studies show that Dbp2 is a functional RNA helicase.[3] This suggests that Dbp2 is a dsRNA-directed ATPase, which targets structured RNA elements *in vivo*.

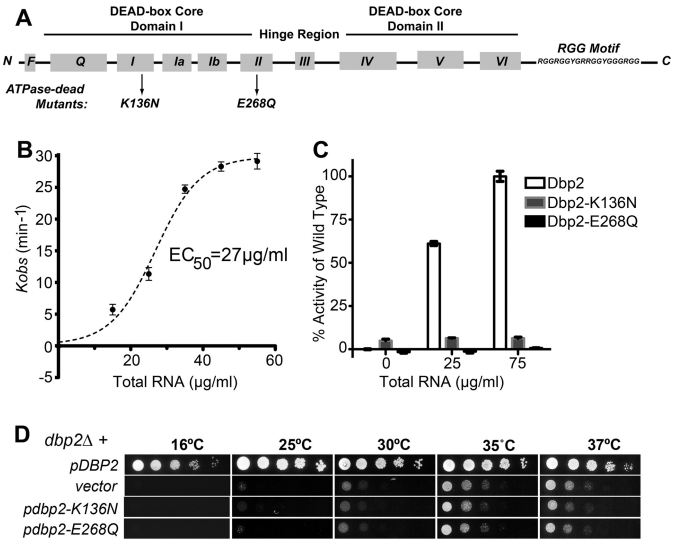

FIGURE 1. **Dbp2 is an RNA-dependent ATPase *in vitro* whose activity is required for normal cell growth.** *A,* schematic representation of Dbp2 primary sequence and conserved DEAD-box protein motifs. Core domains and the 10 sequence motifs are indicated (11). Dbp2 also contains a C-terminal RGG accessory domain predicted to enhance RNA binding activity (33). *Arrows* denote amino acid substitutions in motif I or motif II. *B,* Dbp2 is an enzymatically active, RNA-dependent ATPase *in vitro*. The ability of Dbp2 to hydrolyze ATP was assessed using an absorbance-based *in vitro* ATPase assay as described previously, which measures ATP hydrolysis indirectly through a linear depletion of NADH (20). Assays were conducted with 400 nM of recombinant purified His_6-tagged Dbp2 and increasing amounts of total yeast RNA. ATP turnover numbers (k_{obs}) were calculated from initial velocities of each assay conducted in triplicate. The EC_{50} value for RNA was determined through nonlinear regression analysis and is reflective of the concentration of RNA needed to activate ATP hydrolysis to a half-maximal rate. All data are normalized to background signals that result from very low levels of NADH depletion in buffer alone ($V_0 = 1.01 \pm 0.5$ min^{-1}). The observed ATPase rate of Dbp2 in the absence of RNA is 0.98 ± 0.4 min^{-1}, which is equivalent to buffer alone. *C,* mutation of residues within motif I and II impair enzymatic activity. Recombinant purified His_6-tagged variants Dbp2-K136N or Dbp2-E268Q were assayed for ATP hydrolysis as above using RNA concentrations equal to or 3-fold above the wild type EC_{50} concentration. Enzymatic activities are reported as a percentage of the initial velocity of ATP hydrolysis of wild type Dbp2 with 75 μg/ml RNA. *D, DBP2*-deficient strains display a slow growth and cold-sensitive phenotype. Yeast growth was analyzed using serial dilution analysis of *dbp2*Δ strains transformed with either empty vector alone or CEN plasmids encoding wild type (*pDBP2*) or ATPase-deficient mutants (*pdbp2-K136N* or *pdbp2-E268Q*) as indicated. Strains were subsequently spotted in 5-fold serial dilutions onto selective media and grown for 3–5 days at the indicated temperatures.

Dbp2 Is a Predominantly Nuclear Protein Whose Loss Is Suppressed by 6-Azauracil—Studies of Dbp2 in budding yeast have provided conflicting evidence regarding the precise localization of Dbp2 ranging from nuclear/nucleolar to predominantly cytoplasmic (16, 36). To understand the cellular function(s) of Dbp2, we asked where Dbp2 is localized at steady state by con-

[3] W. K. Ma, unpublished data.

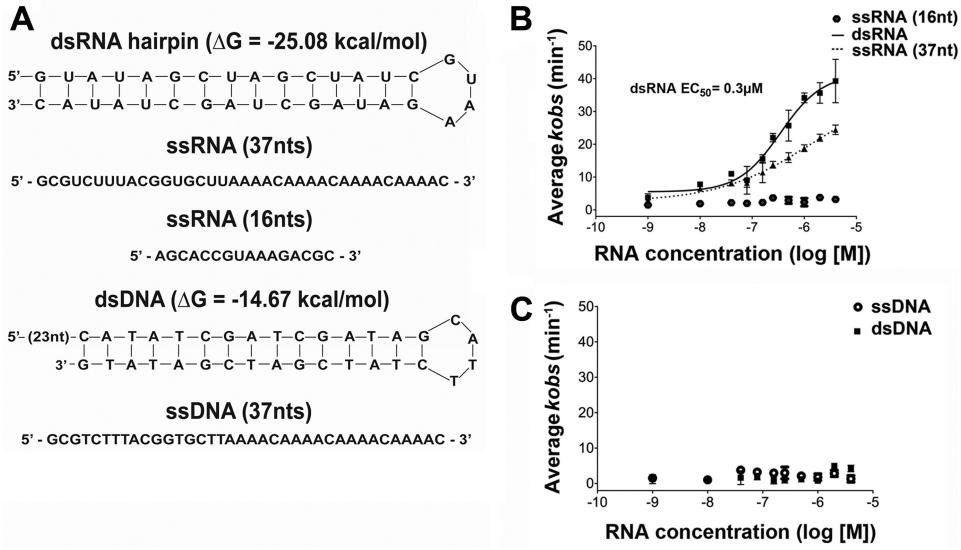

FIGURE 2. **Dbp2 is a dsRNA-directed ATPase *in vitro*.** *A,* sequence and schematic representation of RNA and DNA molecules used below. Δ*G* parameters were calculated using the MFOLD web server. *B,* Dbp2 displays a preference for dsRNA in stimulation of ATP hydrolysis. ATPase assays were conducted as above using purchased single- stranded or double-stranded RNA molecules in *A* at varying concentrations from 1 nM to 4 μM and purified Dbp2 (0.2 μM). ATP hydrolysis activity was determined in triplicate for each nucleic acid concentration and is plotted on a semi-logarithmic graph as k_{obs} *versus* log[M] concentration of RNA. The resulting EC_{50} from the dsRNA hairpin was determined through nonlinear regression analysis. EC_{50} values could not be determined for the single-stranded RNA molecules due to low levels of ATPase stimulation. *C,* ATPase activity of Dbp2 is not stimulated by DNA. *In vitro* ATPase assays were conducted as above with the DNA molecules indicated in *A* using purchased DNA molecules. *nt*, nucleotide.

ducting fluorescent microscopy of a fluorescently tagged *DBP2-GFP* strain harboring a GFP fusion at the endogenous locus. This revealed that Dbp2-GFP is a predominantly nucleoplasmic protein, colocalizing with DAPI-stained DNA, with accumulation in the nucleolus (Fig. 3*A*). This is consistent with the role of Dbp2 in ribosome biogenesis and is suggestive of an additional nuclear function.

To pinpoint a role for Dbp2 in the nucleoplasm, we subsequently asked if loss of *DBP2* renders cells sensitive to transcriptional stress by conducting growth assays of wild type and *dbp2*Δ cells with or without 100 μg/ml 6AU (Fig. 3*B*). 6AU is a transcriptional inhibitor that has been widely utilized to identify genes whose products positively regulate transcription elongation (37). Surprisingly, 6AU partially rescues the slow growth defects of the *dbp2*Δ strain at semi-permissive temperatures of 30 and 32 °C, suggesting that reduction of transcription improves the growth of *DBP2*-deficient strains.

DBP2 Represses Cryptic Initiation within the FLO8 Locus—Interestingly, 6AU resistance or suppression phenotypes have been noted in only a few published reports and correlate with loss of gene products that negatively regulate transcription. This includes the transcriptional regulator/mRNA processing factor, *SSU72*, as well as chromatin-modifying enzymes like the histone methyltransferase *SET2* (38–40). To further characterize the biological role of Dbp2, we asked if *dbp2*Δ strains exhibit transcriptional defects similar to those associated with impaired repression. One type of transcriptional defect is cryptic initiation whereby failure to properly assemble chromatin results in initiation at noncognate sites either within (intragenic) or outside of (intergenic) transcribed genomic loci (28, 41, 42). To determine whether *DBP2* is required for repression of intragenic cryptic initiation, we utilized a previously characterized p*GAL-FLO8*:*HIS3* reporter construct for identification of initiation defects through a simple growth assay (28, 41). We constructed *dbp2*Δ *pGAL-FLO8*:*HIS3* strains and subsequently analyzed growth of two independent isolates with respect to wild type and *spt6-1004* strains as negative and positive controls, respectively. *SPT6* encodes a transcriptional elongation factor whose mutation results in characterized cryptic initiation defects (28, 41). Strikingly, loss of *DBP2* also results in cryptic intragenic initiation (Fig. 3*D*). Unlike *spt6-1004* strains, however, *dbp2*Δ strains require transcriptional induction for detection of cryptic initiation. This suggests that Dbp2 is needed only in the context of active transcriptional activity. Next, we conducted Northern blotting of *FLO8* transcripts from wild type, *dbp2*Δ, and *spt6-1004* strains to determine whether *dbp2*Δ strains also display cryptic initiation at the endogenous *FLO8* gene (Fig. 3*E*). This revealed a small ~4-fold increase in short *FLO8* products in the *dbp2*Δ strain as compared with wild type (4–16%). Thus, *DBP2* is required for repression of cryptic intragenic initiation in the *FLO8* reporter and within the endogenous locus.

GAL7 Transcripts Are Overabundant in the Absence of DBP2—Given that *DBP2*-deficient cells display defects associated with active transcription, we asked if *DBP2* is required for normal expression levels of endogenous genes (Fig. 3*F*). To this end, we selected a panel of genes and assessed transcript abundance in wild type and *dbp2*Δ cells using RT-qPCR. These genes were chosen based on the characterized role of the mammalian Dbp2 ortholog, p68, in cell cycle progression, cell differentiation, and response to extracellular cues (15). This revealed that *GAL7* transcripts are specifically overabundant in *dbp2*Δ cells as compared with wild type, in contrast to other gene products (Fig. 3*F*). Notably, this increase occurs under typical transcriptionally repressive conditions, suggesting that the *GAL7* gene is aberrantly derepressed in *dbp2*Δ cells. Furthermore, there was no detectable difference in *GAL7* transcript levels under

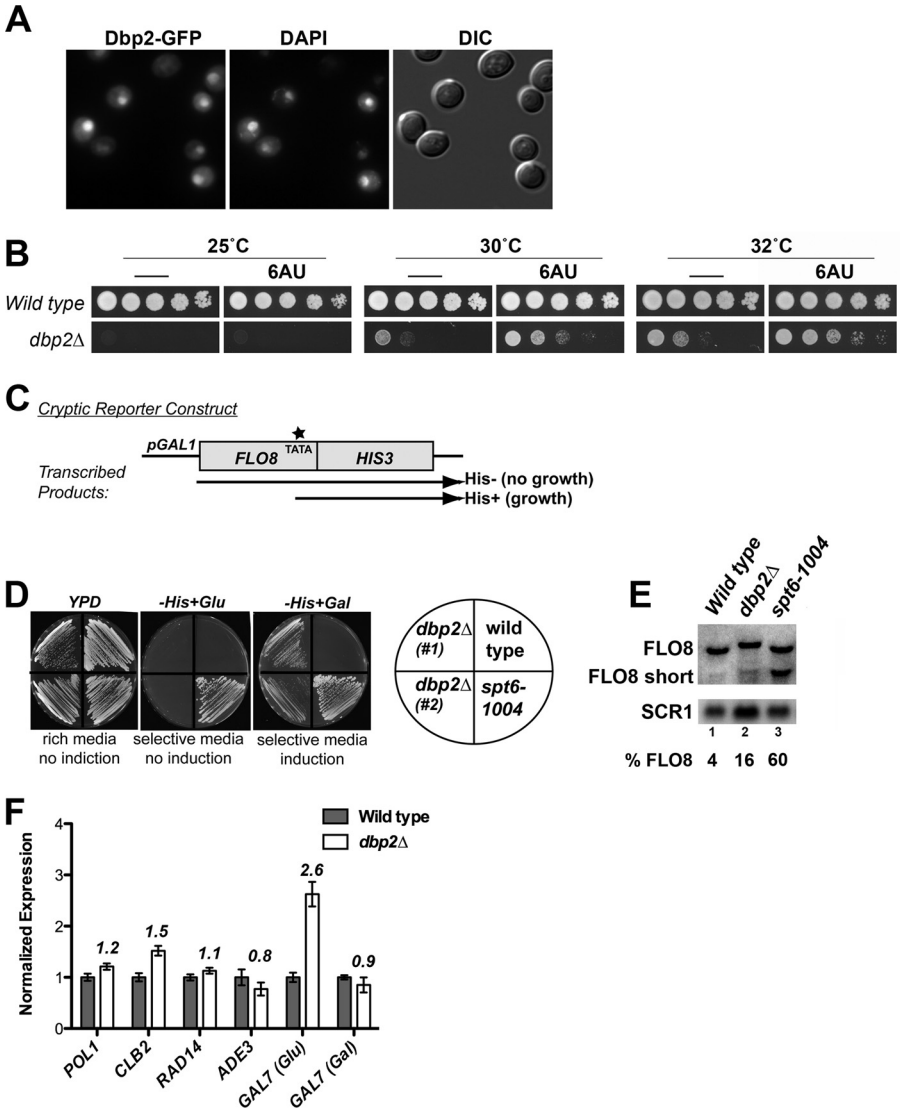

FIGURE 3. **Dbp2 is a predominantly nuclear protein required for repression of cryptic, intragenic initiation within *FLO8* and expression of *GAL7*.** *A,* live cell imaging reveals whole cell distribution of Dbp2 with a predominantly nuclear localization at steady state. Fluorescent microscopy was conducted with exponentially growing *DBP2-GFP* strains grown at 30 °C. Cells were fixed for 1 h with formaldehyde in rich growth media, washed extensively, and stained with DAPI for visualization of DNA. Differential contrast (*DIC*) images are presented in the *right-most panel*. *B,* transcriptional elongation inhibitor, 6AU, partially rescues *dbp2*Δ growth defects. Wild type (BY4741) or *dbp2*Δ strains were analyzed for 6AU sensitivity using serial dilution analysis of strains onto −URA + 2% glucose plates with or without 100 μg/ml 6AU at the indicated temperatures. *C,* schematic diagram of the *FLO8:HIS3* cryptic initiation reporter (adapted from Ref. 28). TATA (*) indicates the approximate position of the cryptic internal start site within the *FLO8* open reading frame. Following induction with galactose (+*Gal*), transcription in wild type cells proceeds through the internal TATA, resulting in out of frame *HIS3* mRNA, and failure to grow on media lacking histidine (−*His* + *Gal*). Defects in chromatin structure or assembly are correlated with aberrant initiation at the internal TATA site, which results in grown on −His media due to production of an in-frame *HIS3* mRNA. *D,* DBP2 is required for repression of cryptic intragenic initiation within the *FLO8:HIS3* reporter gene. Cryptic initiation defects were assessed following construction of *dbp2*Δ strains encoding a chromosomally integrated *pGAL-FLO8:HIS3* reporter. Two independent *dbp2*Δ strain isolates are shown compared with *DBP2* wild type and an *spt6–1004* mutant strain as negative and positive controls, respectively (27, 28). *E,* loss of DBP2 results in an ~4-fold increase in aberrant FLO8 transcripts from the endogenous *FLO8* locus. Briefly, total RNA was isolated from wild type, *dbp2*Δ, and *spt6--1004* strains and subjected to Northern blotting. 30 μg of total RNA was resolved on a 1.2% formaldehyde/agarose gel, transferred to a nylon membrane, and probed with a double-stranded, radiolabeled DNA probe corresponding to both the full-length and short 3′ transcript product. *SCR1* transcripts are shown as a loading control. *F, DBP2* is required to maintain endogenous levels of *GAL7* under transcriptionally repressive conditions (+glucose). The transcript abundance of individual gene products was determined by RT-qPCR analysis of RNA isolated from wild type or *dbp2*Δ strains grown at 35 °C. Transcript levels were determined by quantitative PCR using the Bio-Rad CFX system and SYBR Green with the indicated primer sets (Table 2). Gene product annotations are as follows: *POL1* (DNA primase 1), *CLB2* (cyclin B2), *RAD14* (DNA repair), *ADE3* (nucleotide biosynthesis), and *GAL7* (carbon source metabolism). *GAL7* primers correspond to set *6* in subsequent figures. Differences were calculated using the Pfaffl method (22) and are normalized to the level of *ACT1*. *Error bars* represent the mean ± S.E.

induced conditions (+galactose) between wild type and *dbp2*Δ cells. This suggests that Dbp2 is required for both repression of cryptic intragenic initiation and of normal promoter elements of protein-coding genes.

Dbp2 Associates Directly with Chromatin, Correlating with Transcriptional Activity—The *GAL* cluster is a well established model for dissection of gene regulatory mechanisms in *S. cerevisiae*. Briefly, the *GAL* genes are considered to have three transcriptional states as follows: active (+galactose), derepressed (+raffinose), and repressed (+glucose) (43). In the presence of galactose, transcriptional activation proceeds via the transcription factor Gal4. In the repressed state, transcriptional repressors Nrg1 and Mig1/Mig2 are responsible for promoting glucose-dependent repression (43, 44).

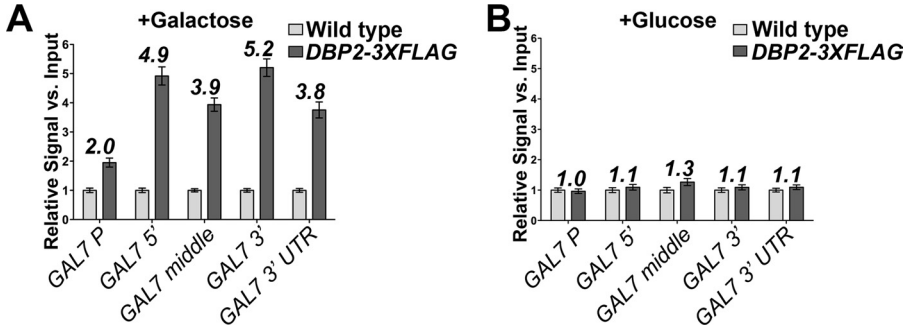

FIGURE 4. **Dbp2–3×FLAG is recruited to the *GAL7* open reading frame in a transcriptionally dependent manner.** *A,* Dbp2 associates with the *GAL7* locus, predominantly within the coding region and 3′UTR. Chromatin immunoprecipitation (*ChIP*) experiments were conducted with strains expressing untagged or C-terminally 3×FLAG-tagged Dbp2 from the endogenous locus grown in rich media after a 5-h transcriptional induction (+*galactose*). Bound DNA was detected by qPCR using primer sets corresponding to the indicated genomic locations (see Table 5). Resulting signals are reported as the relative signal above an untagged wild type strain with respect to input and are the result of three independent biological replicates with three technical repeats. *Numbers* above each bar represent the average difference above background (untagged strain). *Error bars* indicate S.E. as above. *B,* Dbp2–3×FLAG is not detectibly associated with GAL7 under transcriptionally repressive conditions. ChIP-qPCR analysis was conducted as in *A* with yeast strains grown in glucose (repressive) conditions.

Our results suggest that *DBP2* is required for proper repression of *GAL7* under transcriptionally repressive conditions, drawing parallels between Dbp2 and glucose-dependent repressors. If this is the case, this would suggest that Dbp2 functions at the *GAL7* and *FLO8* loci through distinctly different mechanisms. To test this, we utilized chromatin immunoprecipitation (ChIP) to determine whether a 3×FLAG-tagged Dbp2 is directly bound to *GAL7* under transcriptionally repressive conditions. Strikingly, this resulted in detection of Dbp2 at the *GAL7* locus under transcriptionally active conditions, in contrast to our predictions (Fig. 4*A*). Dbp2–3×FLAG associates with similar levels ~5-fold above background across the *GAL7* open reading frame with slightly lower association at the promoter region, suggesting recruitment throughout the transcriptional unit (Fig. 4*A*). We were not able to detect appreciable accumulation of Dbp2 at any tested region under repressive conditions (Fig. 4*B*, *+glucose*). Thus, Dbp2 is associated with chromatin in a transcriptionally dependent manner, suggestive of association with the transcriptional machinery and/or nascent RNAs. This also indicates the *GAL7* derepression defect in *dbp2*Δ cells may be due to either an indirect effect or to transcriptional activity, which is below the ChIP detection limit for Dbp2.

DBP2-deficient Cells Display Expression Defects across GAL10-GAL7—The *GAL7* gene is a member of the *GAL1-GAL10-GAL7* gene cluster (Fig. 5*A*). In addition to proteinaceous transcription factors, the *GAL* cluster is also associated with overlapping lncRNAs with estimated levels as low as one molecule in 14 cells (29). These include the well characterized *GAL10* lncRNA (29, 45, 46) and a recently identified, sense-oriented *GAL10s* lncRNA (termed *XUT 109-2m* in Ref. 3).

To determine the origin of the *GAL7* transcriptional product in *dbp2*Δ cells under repressive conditions, we conducted a high resolution RT-qPCR analysis by positioning qPCR primer pairs at the 5′ end of *GAL1*, 5′, middle, and 3′ end of *GAL10*, intragenic region between *GAL10* and *GAL7*, and the 5′, middle, and 3′ region of *GAL7* (Fig. 5*A*, *1–8*). Consistent with our original RT-qPCR analysis above, we detected a 2.5-fold increase at the 5′ end of *GAL7* in *dbp2*Δ (Fig. 5*B*, *6*) and similar increases across the *GAL7* open reading frame indicative of low level expression of the *GAL7* protein-coding gene. Unexpectedly, we also detected a 2-fold increase in transcript abundance upstream of *GAL7*. This is in contrast to the 5′ ends of *GAL1* and *GAL10*, which were not significantly different in wild type *versus dbp2*Δ (Fig. 5*B*, *1*). Next, we conducted RT-qPCR analysis at the *dbp2*Δ semi-permissive temperature of 30 °C with the idea that growth at lower temperatures would thermodynamically "trap" Dbp2-dependent substrates (Fig. 5*C*). Strikingly, this revealed a sharp increase in transcript abundance to ~5-fold above wild type across the same genomic region. This pattern is consistent with aberrant expression across the *GAL7* and *GAL10s* lncRNA coding regions, the latter of which is indicative of a defect in RNA quality control (3).

DBP2-deficient Cells Accumulate Aberrant GAL7 RNAs—To further characterize the role of Dbp2 at the *GAL7* locus, we conducted Northern blotting to visualize *GAL7* transcripts under repressive conditions in wild type and *dbp2*Δ cells at 30 °C (Fig. 6*A*). This revealed a weak but detectable accumulation of transcripts corresponding to both the *GAL7* protein-coding gene and a weak ~2.5-kb product in the *dbp2*Δ strain (Fig. 6*A*, *lanes 4–6*). The latter product most likely corresponds to a 3′-extended *GAL10s* lncRNA that terminates at the end of the *GAL7* gene. This is suggestive of aberrant expression of two *GAL* cluster gene products in *dbp2*Δ cells under normally repressive conditions.

Next, we analyzed the *GAL7* transcripts produced during transcriptional activation in *dbp2*Δ cells at 30 °C (Fig. 6*B*). Strikingly, in addition to abundant expression of *GAL7* mRNA transcripts, which accumulated to similar levels between wild type and *dbp2*Δ, we also detected an ~4-kb product in *DBP2*-deficient cells (Fig. 6*B*, *lanes 4–6*). The 4-kb transcript is consistent with expression of a *GAL10-GAL7* bicistronic mRNA that results from aberrant pre-mRNA processing in other mutant yeast strains (30, 47, 48). Interestingly, we did not detect defects in *dbp2*Δ cells grown at 35 °C, suggesting that higher temperatures partially bypass the requirement for Dbp2 (Fig. 3*F* and data not shown). This is consistent with a general role for Dbp2 in cotranscriptional RNA folding and/or assembly.

GAL7 Transcripts Are a Result of Cryptic Initiation in DBP2-deficient Cells—Given that *GAL7* transcription is induced by the action of a galactose-dependent transcription factor, Gal4 (43), we were surprised at our detection of *GAL7* mRNAs in

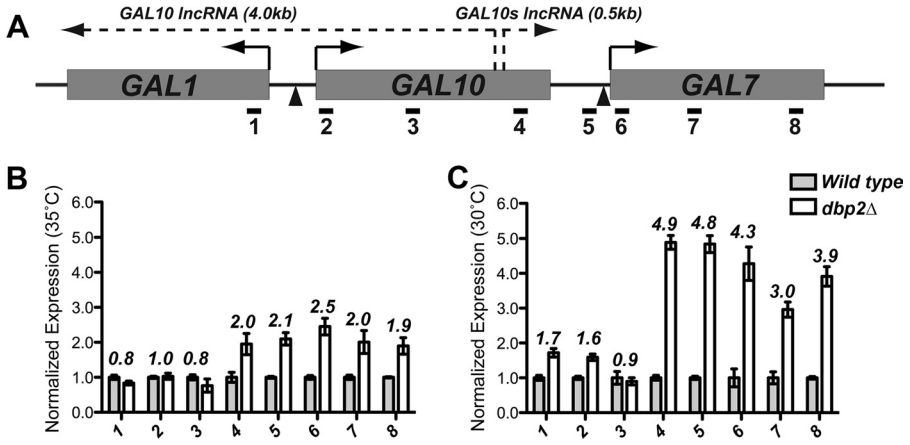

FIGURE 5. ***GAL7* expression is a result of transcriptional defects across the *GAL10-GAL7* genomic region in *DBP2*-deficient cells.** *A,* schematic representation of the GAL operon in *S. cerevisiae* denoting the three galactose-dependent genes (*GAL1*, *GAL10,* and *GAL7*) and previously identified noncoding RNAs (3, 29). *Short solid-line arrows* denote the direction of protein-coding (sense) transcription, and lncRNA transcription is represented by a *dotted line*. *Triangles below* the genes denote approximate positions of promoter elements, and *short horizontal lines* demonstrate positions of primer sets utilized in qPCR (Table 2). Set *6* is the same set used for detection of *GAL7* in Fig. 2. *B,* high resolution RT-qPCR reveals accumulation of the *GAL10s* lncRNA and transcription through the *GAL7* ORF. RT-qPCR was conducted as in Fig. 2 using higher resolution qPCR primer pairs (Table 2) with strains grown at 35 °C. *C,* growth at the *dbp2*Δ semi-permissive temperature of 30 °C exacerbates *GAL7* expression defects. High resolution RT-qPCR was conducted as above using wild type or *dbp2*Δ strains grown at 30 °C.

repressive conditions when Gal4 is inactive. To determine whether the *GAL7* transcripts originate from the normal +1 transcriptional start site, we utilized 5′RACE to map the 5′ ends of *GAL7* sense transcripts in *DBP2*-deficient cells. Strikingly, this revealed that the *GAL7* transcripts are aberrant with respect to the wild type initiation site (Fig. 6*C*). Whereas transcriptional induction in wild type cells by addition of galactose results in a single PCR product of ~500 bp, transcripts in the *dbp2*Δ cells are distinct from normal *GAL7* mRNAs (Fig. 6*C*, *lanes 1* and *2*). Sequencing of the resulting PCR products revealed the following three distinct transcriptional start sites in the *dbp2*Δ strain: one intergenic site at −50 bp upstream of the +1 start site, corresponding to two PCR products due to 5′RACE efficiency; and two intragenic sites within the open reading frame of *GAL7* (Fig. 6*D*). In contrast, 5′RACE analysis of *GAL7* mRNAs under activated conditions revealed identical transcriptional start sites between wild type and *dbp2*Δ cells (data not shown). Thus, the *GAL7* transcripts in *dbp2*Δ cells under repressive conditions are a result of cryptic intragenic initiation with respect to the *GAL10s* lncRNA, consistent with the requirement for *DBP2* at the *FLO8* locus. We speculate that the cryptic initiation defects in *DBP2*-deficient cells are an indirect result of failure to "clear" aberrant RNAs rather than a direct role in chromatin assembly, given the recent connections between RNA quality control and chromatin architecture (see "Discussion").

Simultaneous Loss of DBP2 and RRP6 Results in a Lethal Growth Phenotype—Major factors in RNA quality control are the nuclear exosome component, *RRP6,* and the cytoplasmic exonuclease, *XRN1* (2, 3). To gain further insight into the biochemical pathway for *DBP2* function, we conducted synthetic genetic analysis of *dbp2*Δ and *xrn1*Δ or *rrp6*Δ alleles using a plasmid shuffle assay (Fig. 7). This assay exploits the toxic effects of 5-fluoroorotic acid in strains that cannot grow in the absence of a plasmid encoding the uracil biosynthesis gene (*URA3*) and wild type *DBP2* (p*DBP2*). Strikingly, this revealed that *rrp6*Δ and *dbp2*Δ are synthetic lethal at all growth temperatures (Fig. 7). This genetic interaction is specific, as a *dbp2*Δ *xrn1*Δ strain grows well in the absence of the p*DBP2*. This supports a role for Dbp2 in RNA quality control steps in the nucleus. More importantly, this shows that Dbp2 is a major factor in RNA quality control that likely plays roles at multiple genes outside of the *GAL7* and *FLO8.* Taken together, we provide a model whereby the DEAD-box protein Dbp2 functions at the interface of chromatin and RNA quality control to modulate RNA structure in a manner that promotes both downstream processing steps and reassembly of chromatin in the wake of active transcription (Fig. 8). This suggests that Dbp2 is a cotranscriptional RNA chaperone, central to fidelity of the gene expression network.

DISCUSSION

A major challenge to the RNA biology field is understanding how the RNA and RNP structure contributes to cellular processes. The DEAD-box RNA helicases are central players in RNP dynamics, functioning in all aspects of RNA metabolism through ATP-dependent modulation of RNA structures (11). These include the DEAD-box proteins Sub2 and Dbp5, which are required for mRNP packing and nuclear export, respectively (49–51). Our studies now elucidate Dbp2 as a critical factor in transcriptional fidelity, adding to the complement of DEAD-box proteins associated with maintenance of the transcriptome. Furthermore, our studies provide provocative evidence that Dbp2 functions as a cotranscriptional RNA chaperone. This would be consistent with current models for DEAD-box proteins as ATP-dependent chaperones and with elegant *in vitro* studies that support this mechanism (14, 52, 53).

With elucidation of Dbp2 as a key player in this process, several tantalizing questions now emerge regarding the precise biochemical mechanism in gene regulation. Our results suggest that Dbp2 is a dsRNA-dependent ATPase recruited to chromatin during transcription. Furthermore, our studies show that *DBP2* is genetically linked to the nuclear exosome component, *RRP6*. It is well established that Rrp6-dependent decay of

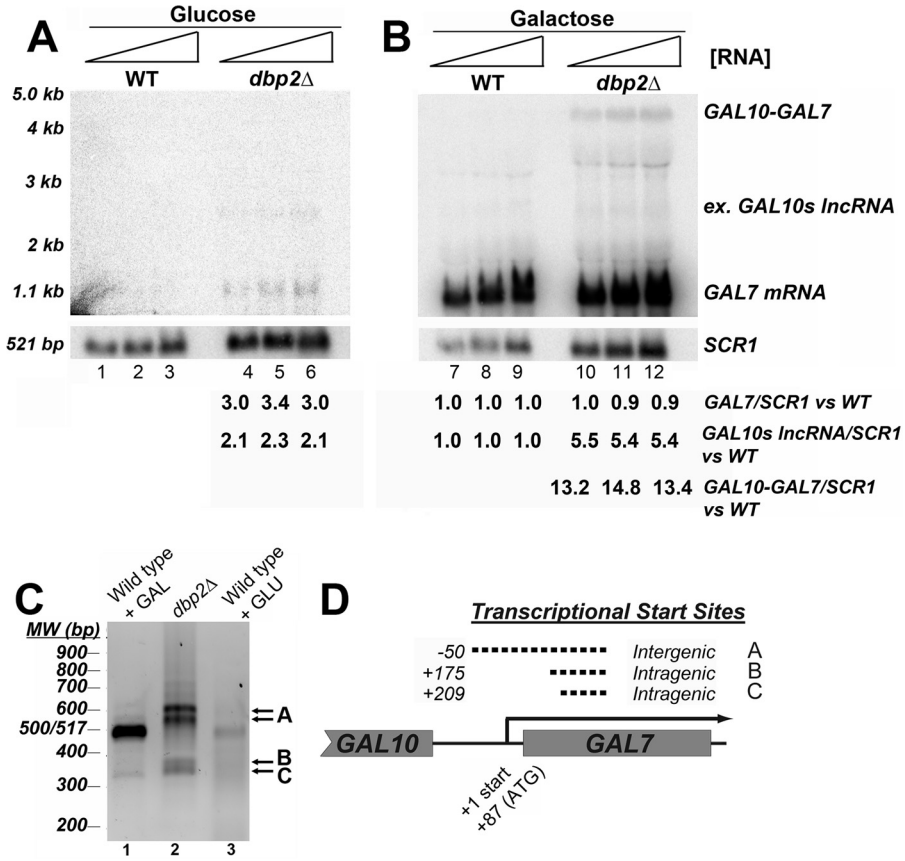

FIGURE 6. **Loss of *DBP2* results in cryptic initiation at *GAL7* and termination defects within the *GAL10-GAL7* region under repressed and activated conditions, respectively.** *A,* Northern blotting of total RNA from wild type and *dbp2*Δ cells reveals expression of *GAL7* and a 3′-extended *GAL10s* lncRNA under typically repressive conditions. Northern blotting was conducted with increasing amounts of total RNA (20–50 μg) from indicated strains grown at the semi-permissive *dbp2*Δ temperature of 30 °C in glucose (repressive) conditions (*lanes 1–6*). Accumulation of *GAL7* mRNA and a 2.5-kb transcript, likely corresponding to a 3′ extended *GAL10s* lncRNA, is evident in *lanes 4–6*. Other products at ~2 and 3.5 kb are background detection of 18 S and 25 S rRNA. Quantification is provided *below* each lane and corresponds to the quantity of the indicated transcript *versus* wild type normalized to levels of SCR1 for each lane. In lanes with no detectable product, quantities were normalized to background. *B,* transcriptional induction of the *GAL* genes results in expression of *GAL7* and appearance of a *GAL10–GAL7* transcript. Northern blotting was conducted as above following a 5-h shift to galactose-containing media. Under transcriptionally induced conditions, *GAL7* mRNA is induced along with an ~4-kb product, which most likely corresponds to a *GAL10-GAL7* bicistronic mRNA (*lanes 10–12*). *C, GAL7* mRNA transcripts in *dbp2*Δ strains are aberrant with respect to wild type *GAL7* products. Resulting 5′RACE products of aberrant *dbp2*Δ transcripts (*lane 2*) are shown with respect to the induced wild type *GAL7* transcript (*lane 1*) and basal transcriptional products (*lane 3*) shown following resolution on a 1.3% agarose gel and visualization by ethidium bromide staining. The three most prominent 5′RACE products in the *dbp2*Δ cells are denoted *A–C* to the *right* of the gel. The two A bands correspond to the same transcription initiation site (as determined by sequencing) and are likely due to differences in the cDNA "tailing" efficiency in the 5′RACE. Note that these experiments are not quantitative and do not reflect relative transcript abundance between strains or conditions. *D, GAL7* transcripts are the result of cryptic initiation events in the *dbp2*Δ strain under typically repressive conditions. Schematic representation of *GAL7* transcriptional start sites in *DBP2*-deficient cells as determined following cloning and sequencing of resulting 5′RACE products. *Dotted lines* denote cryptic transcriptional elements between (inter) or within (intra) an open reading frame with respect to the normal +1 start site in transcriptionally induced wild type cells (*solid line*) (74).

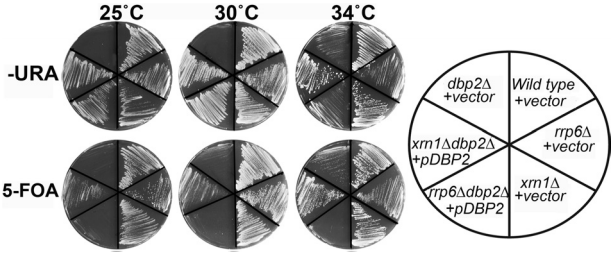

FIGURE 7. **Simultaneous loss of *DBP2* and the nuclear RNA decay factor, *RRP6*, results in synthetic lethality.** Synthetic growth defects were measured using a plasmid shuffle assay, which exploits the ability of yeast to grow in the absence of a *URA3*-encoding plasmid (vector or p*DBP2*). Indicated strains were constructed using standard yeast manipulations, and resulting transformants were streaked on either −URA or 5-fluoroorotic acid media to demonstrate growth in the presence or absence of plasmid-encoded *DBP2*, respectively.

numerous noncoding RNAs is dependent on transcription termination mechanisms (54). The primary mechanism for termination of short noncoding transcripts is through the Nrd1-Sen1 pathway whereby RNA-binding proteins, Nrd1 and Nab3, recognize specific RNA sequences in nascent RNA transcripts (55–57). Thus, it is tempting to speculate that Dbp2 promotes loading of RNA-binding proteins, such as Nrd1 and Nab3, by resolving inhibitory RNA structures. This is consistent with accumulation of a putative *GAL10-GAL7* read-through transcript in *dbp2*Δ cells and with identification of an Nrd1-dependent termination mechanism at the *GAL10* gene (47). However, given the pattern of *Dbp2* gene association and the requirement for repression of initiation, the role of Dbp2 is not likely limited to recruitment of these two factors. Interestingly, studies have also shown that the genes within the *GAL* cluster are associated with gene looping events between promoters and terminators

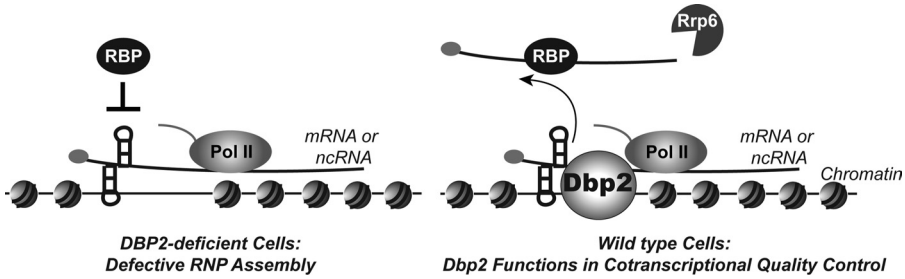

FIGURE 8. **Dbp2 is a dsRNA-directed DEAD-box enzyme that functions in cotranscriptional RNA quality control.** Our results document a previously unrecognized role for Dbp2 in transcriptional quality control. We suggest that Dbp2 is recruited during transcription to promote clearance of newly transcribed RNA from genomic loci, whose presence interferes with both chromatin and mRNP assembly. This activity may involve direct modulation of RNA or RNP structures to promote association of RNA-binding proteins (*RBPs*) such as factors required for RNA processing and/or decay. This activity would also be predicted to inhibit further synthesis of aberrant cryptic transcripts through reformation of chromatin architecture, consistent with recent studies of other cotranscriptional RNA processing/assembly factors (63, 65). *Pol II,* polymerase II.

(58–60). These gene loops have been shown to influence the rate of transcriptional reactivation in a process termed "transcriptional memory" (61). It will be interesting to determine whether Dbp2 and/or RNA folding influence higher order chromatin architecture.

Because loss of *DBP2* results in cryptic transcription indicative of aberrant chromatin architecture, we suggest that the activity of Dbp2 is necessary to promote clearance of nascent RNAs from genomic loci. Furthermore, we speculate that this requirement is due to the presence of RNA structures within nascent transcripts, which would be predicted to impair RNA processing and RNP complex assembly. In line with this model, strains deficient in cotranscriptional mRNP processing and packaging accumulate RNA:DNA hybrids in structures termed R-loops, which induce multiple defects associated with aberrant chromatin architecture (62–66). For example, simultaneous loss of the TRAMP component Trf4 and histone deacetylase Sir2 results in severe ribosomal DNA instability, underscoring an intimate connection between maintenance of the genome and transcriptome (67).

It is well understood that the activity of RNA polymerases is dependent on the chromatin environment. Moreover, loss of chromatin remodeling or histone modification machinery results in aberrant transcription, including cryptic transcriptional initiation both between and within the gene loci (28, 41, 68). To the best of our knowledge, however, no RNA decay or processing factors have been linked specifically to repression of cryptic initiation. Instead, genes encoding histones, histone-modifying enzymes, and chromatin remodeling factors as well as transcription factors have been linked to this activity, supporting the fact that aberrant transcriptional initiation is a result of altered chromatin structure (28). This suggests that either Dbp2 plays a distinct role as a bridging factor between nascent RNAs and chromatin or that roles in repressing cryptic initiation have not been defined thus far for other RNA processing factors.

In mammals, p68 has been linked to numerous cotranscriptional processing steps and has been suggested to associate with dsRNA both *in vitro* and *in vivo*, consistent with the idea that Dbp2 cotranscriptionally modulates RNA structures (34, 69, 70). Thus, the role of Dbp2 is likely evolutionarily conserved with future studies providing key insights into the biochemical mechanisms in eukaryotic gene regulation. More importantly, however, numerous studies have shown that p68 is a potent oncogene whose overexpression results in chemotherapeutic resistance (71, 72). In summary, our studies uncover a role for Dbp2 at the interface of RNA surveillance and chromatin architecture as a missing link in quality control of the transcriptome.

Acknowledgments—We thank Joe Ogas, Barb Golden, and Scott Briggs for constructive criticism regarding this manuscript. We also thank members of the Scott Briggs laboratory for assistance with experimental methods. Finally, we thank members of the Tran laboratory for scientific discussions.

REFERENCES

1. Moore, M. J., and Proudfoot, N. J. (2009) Pre-mRNA processing reaches back to transcription and ahead to translation. *Cell* **136,** 688–700
2. Neil, H., Malabat, C., d'Aubenton-Carafa, Y., Xu, Z., Steinmetz, L. M., and Jacquier, A. (2009) Widespread bidirectional promoters are the major source of cryptic transcripts in yeast. *Nature* **457,** 1038–1042
3. van Dijk, E. L., Chen, C. L., d'Aubenton-Carafa, Y., Gourvennec, S., Kwapisz, M., Roche, V., Bertrand, C., Silvain, M., Legoix-Né, P., Loeillet, S., Nicolas, A., Thermes, C., and Morillon, A. (2011) XUTs are a class of Xrn1-sensitive antisense regulatory noncoding RNA in yeast. *Nature* **475,** 114–117
4. Cabili, M. N., Trapnell, C., Goff, L., Koziol, M., Tazon-Vega, B., Regev, A., and Rinn, J. L. (2011) Integrative annotation of human large intergenic noncoding RNAs reveals global properties and specific subclasses. *Genes Dev.* **25,** 1915–1927
5. Berretta, J., and Morillon, A. (2009) Pervasive transcription constitutes a new level of eukaryotic genome regulation. *EMBO Rep.* **10,** 973–982
6. Wang, K. C., and Chang, H. Y. (2011) Molecular mechanisms of long noncoding RNAs. *Mol. Cell* **43,** 904–914
7. Schmid, M., and Jensen, T. H. (2010) Nuclear quality control of RNA polymerase II transcripts. *Wiley Interdiscip. Rev. RNA* **1,** 474–485
8. Libri, D., Dower, K., Boulay, J., Thomsen, R., Rosbash, M., and Jensen, T. H. (2002) Interactions between mRNA export commitment, 3′ end quality control, and nuclear degradation. *Mol. Cell. Biol.* **22,** 8254–8266
9. Rougemaille, M., Gudipati, R. K., Olesen, J. R., Thomsen, R., Seraphin, B., Libri, D., and Jensen, T. H. (2007) Dissecting mechanisms of nuclear mRNA surveillance in THO-sub2 complex mutants. *EMBO J.* **26,** 2317–2326
10. Galy, V., Gadal, O., Fromont-Racine, M., Romano, A., Jacquier, A., and Nehrbass, U. (2004) Nuclear retention of unspliced mRNAs in yeast is mediated by perinuclear Mlp1. *Cell* **116,** 63–73
11. Linder, P., and Jankowsky, E. (2011) From unwinding to clamping. The DEAD-box RNA helicase family. *Nat. Rev. Mol. Cell Biol.* **12,** 505–516
12. Fairman, M. E., Maroney, P. A., Wang, W., Bowers, H. A., Gollnick, P., Nilsen, T. W., and Jankowsky, E. (2004) Protein displacement by

DE*X*(H/D) "RNA helicases" without duplex unwinding. *Science* **304,** 730–734
13. Del Campo, M., Mohr, S., Jiang, Y., Jia, H., Jankowsky, E., and Lambowitz, A. M. (2009) Unwinding by local strand separation is critical for the function of DEAD-box proteins as RNA chaperones. *J. Mol. Biol.* **389,** 674–693
14. Bhaskaran, H., and Russell, R. (2007) Kinetic redistribution of native and misfolded RNAs by a DEAD-box chaperone. *Nature* **449,** 1014–1018
15. Janknecht, R. (2010) Multitalented DEAD-box proteins and potential tumor promoters. p68 RNA helicase (DDX5) and its paralog, p72 RNA helicase (DDX17). *Am. J. Transl. Res.* **2,** 223–234
16. Bond, A. T., Mangus, D. A., He, F., and Jacobson, A. (2001) Absence of Dbp2p alters both non-sense-mediated mRNA decay and rRNA processing. *Mol. Cell. Biol.* **21,** 7366–7379
17. Nissan, T. A., Bassler, J., Petfalski, E., Tollervey, D., and Hurt, E. (2002) 60 S pre-ribosome formation viewed from assembly in the nucleolus until export to the cytoplasm. *EMBO J.* **21,** 5539–5547
18. Barta, I., and Iggo, R. (1995) Autoregulation of expression of the yeast Dbp2p "DEAD-box" protein is mediated by sequences in the conserved DBP2 intron. *EMBO J.* **14,** 3800–3808
19. Banroques, J., Cordin, O., Doère, M., Linder, P., and Tanner, N. K. (2008) A conserved phenylalanine of motif IV in superfamily 2 helicases is required for cooperative, ATP-dependent binding of RNA substrates in DEAD-box proteins. *Mol. Cell. Biol.* **28,** 3359–3371
20. Noble, K. N., Tran, E. J., Alcázar-Román, A. R., Hodge, C. A., Cole, C. N., and Wente, S. R. (2011) The Dbp5 cycle at the nuclear pore complex during mRNA export II. Nucleotide cycling and mRNP remodeling by Dbp5 are controlled by Nup159 and Gle1. *Genes Dev.* **25,** 1065–1077
21. Johnson, S. A., Cubberley, G., and Bentley, D. L. (2009) Cotranscriptional recruitment of the mRNA export factor Yra1 by direct interaction with the 3′ end processing factor Pcf11. *Mol. Cell* **33,** 215–226
22. Pfaffl, M. W. (2001) A new mathematical model for relative quantification in real time RT-PCR. *Nucleic Acids Res.* **29,** e45
23. Güldener, U., Heck, S., Fielder, T., Beinhauer, J., and Hegemann, J. H. (1996) A new efficient gene disruption cassette for repeated use in budding yeast. *Nucleic Acids Res.* **24,** 2519–2524
24. Sikorski, R. S., and Hieter, P. (1989) A system of shuttle vectors and yeast host strains designed for efficient manipulation of DNA in *Saccharomyces cerevisiae*. *Genetics* **122,** 19–27
25. Gelbart, M. E., Rechsteiner, T., Richmond, T. J., and Tsukiyama, T. (2001) Interactions of Isw2 chromatin remodeling complex with nucleosomal arrays. Analyses using recombinant yeast histones and immobilized templates. *Mol. Cell. Biol.* **21,** 2098–2106
26. Hartzog, G. A., Wada, T., Handa, H., and Winston, F. (1998) Evidence that Spt4, Spt5, and Spt6 control transcription elongation by RNA polymerase II in *Saccharomyces cerevisiae*. *Genes Dev.* **12,** 357–369
27. Prather, D., Krogan, N. J., Emili, A., Greenblatt, J. F., and Winston, F. (2005) Identification and characterization of Elf1, a conserved transcription elongation factor in *Saccharomyces cerevisiae*. *Mol. Cell. Biol.* **25,** 10122–10135
28. Cheung, V., Chua, G., Batada, N. N., Landry, C. R., Michnick, S. W., Hughes, T. R., and Winston, F. (2008) Chromatin- and transcription-related factors repress transcription from within coding regions throughout the *Saccharomyces cerevisiae* genome. *PLoS Biol.* **6,** e277
29. Houseley, J., Rubbi, L., Grunstein, M., Tollervey, D., and Vogelauer, M. (2008) An ncRNA modulates histone modification and mRNA induction in the yeast GAL gene cluster. *Mol. Cell* **32,** 685–695
30. Greger, I. H., and Proudfoot, N. J. (1998) Poly(A) signals control both transcriptional termination and initiation between the tandem *GAL10* and *GAL7* genes of S*accharomyces cerevisiae*. *EMBO J.* **17,** 4771–4779
31. Nagalakshmi, U., Wang, Z., Waern, K., Shou, C., Raha, D., Gerstein, M., and Snyder, M. (2008) The transcriptional landscape of the yeast genome defined by RNA sequencing. *Science* **320,** 1344–1349
32. Yassour, M., Kaplan, T., Fraser, H. B., Levin, J. Z., Pfiffner, J., Adiconis, X., Schroth, G., Luo, S., Khrebtukova, I., Gnirke, A., Nusbaum, C., Thompson, D. A., Friedman, N., and Regev, A. (2009) *Ab initio* construction of a eukaryotic transcriptome by massively parallel mRNA sequencing. *Proc. Natl. Acad. Sci. U.S.A.* **106,** 3264–3269
33. Banroques, J., Cordin, O., Doère, M., Linder, P., and Tanner, N. K. (2011) Analyses of the functional regions of DEAD-box RNA "helicases" with deletion and chimera constructs tested *in vivo* and *in vitro*. *J. Mol. Biol.* **413,** 451–472
34. Huang, Y., and Liu, Z. R. (2002) The ATPase, RNA unwinding, and RNA binding activities of recombinant p68 RNA helicase. *J. Biol. Chem.* **277,** 12810–12815
35. Cordin, O., Banroques, J., Tanner, N. K., and Linder, P. (2006) The DEAD-box protein family of RNA helicases. *Gene* **367,** 17–37
36. Huh, W. K., Falvo, J. V., Gerke, L. C., Carroll, A. S., Howson, R. W., Weissman, J. S., and O'Shea, E. K. (2003) Global analysis of protein localization in budding yeast. *Nature* **425,** 686–691
37. Riles, L., Shaw, R. J., Johnston, M., and Reines, D. (2004) Large scale screening of yeast mutants for sensitivity to the IMP dehydrogenase inhibitor 6-azauracil. *Yeast* **21,** 241–248
38. Keogh, M. C., Kurdistani, S. K., Morris, S. A., Ahn, S. H., Podolny, V., Collins, S. R., Schuldiner, M., Chin, K., Punna, T., Thompson, N. J., Boone, C., Emili, A., Weissman, J. S., Hughes, T. R., Strahl, B. D., Grunstein, M., Greenblatt, J. F., Buratowski, S., and Krogan, N. J. (2005) Cotranscriptional set2 methylation of histone H3 lysine 36 recruits a repressive Rpd3 complex. *Cell* **123,** 593–605
39. Dichtl, B., Blank, D., Ohnacker, M., Friedlein, A., Roeder, D., Langen, H., and Keller, W. (2002) A role for SSU72 in balancing RNA polymerase II transcription elongation and termination. *Mol. Cell* **10,** 1139–1150
40. Du, H. N., and Briggs, S. D. (2010) A nucleosome surface formed by histone H4, H2A, and H3 residues is needed for proper histone H3 Lys-36 methylation, histone acetylation, and repression of cryptic transcription. *J. Biol. Chem.* **285,** 11704–11713
41. Kaplan, C. D., Laprade, L., and Winston, F. (2003) Transcription elongation factors repress transcription initiation from cryptic sites. *Science* **301,** 1096–1099
42. Quan, T. K., and Hartzog, G. A. (2010) Histone H3K4 and K36 methylation, Chd1 and Rpd3S oppose the functions of *Saccharomyces cerevisiae* Spt4-Spt5 in transcription. *Genetics* **184,** 321–334
43. Sellick, C. A., Campbell, R. N., and Reece, R. J. (2008) Galactose metabolism in yeast structure and regulation of the Leloir pathway enzymes and the genes encoding them. *Int. Rev. Cell Mol. Biol.* **269,** 111–150
44. Zhou, H., and Winston, F. (2001) NRG1 is required for glucose repression of the *SUC2* and *GAL* genes of *Saccharomyces cerevisiae*. *BMC Genet.* **2,** 5
45. Geisler, S., Lojek, L., Khalil, A. M., Baker, K. E., and Coller, J. (2012) Decapping of long noncoding RNAs regulates inducible genes. *Mol. Cell* **45,** 279–291
46. Pinskaya, M., Gourvennec, S., and Morillon, A. (2009) H3 lysine 4 di- and tri-methylation deposited by cryptic transcription attenuates promoter activation. *EMBO J.* **28,** 1697–1707
47. Rondón, A. G., Mischo, H. E., Kawauchi, J., and Proudfoot, N. J. (2009) Fail-safe transcriptional termination for protein-coding genes in *S. cerevisiae*. *Mol. Cell* **36,** 88–98
48. Kaplan, C. D., Holland, M. J., and Winston, F. (2005) Interaction between transcription elongation factors and mRNA 3′ end formation at the *Saccharomyces cerevisiae* GAL10-GAL7 locus. *J. Biol. Chem.* **280,** 913–922
49. Tran, E. J., Zhou, Y., Corbett, A. H., and Wente, S. R. (2007) The DEAD-box protein Dbp5 controls mRNA export by triggering specific RNA:protein remodeling events. *Mol. Cell* **28,** 850–859
50. Strässer, K., Masuda, S., Mason, P., Pfannstiel, J., Oppizzi, M., Rodriguez-Navarro, S., Rondón, A. G., Aguilera, A., Struhl, K., Reed, R., and Hurt, E. (2002) TREX is a conserved complex coupling transcription with messenger RNA export. *Nature* **417,** 304–308
51. Fasken, M. B., and Corbett, A. H. (2009) Mechanisms of nuclear mRNA quality control. *RNA Biol.* **6,** 237–241
52. Jarmoskaite, I., and Russell, R. (2011) DEAD-box proteins as RNA helicases and chaperones. *Wiley Interdiscip. Rev. RNA* **2,** 135–152
53. Sinan, S., Yuan, X., and Russell, R. (2011) The Azoarcus group I intron ribozyme misfolds and is accelerated for refolding by ATP-dependent RNA chaperone proteins. *J. Biol. Chem.* **286,** 37304–37312
54. Rougemaille, M., and Libri, D. (2011) Control of cryptic transcription in eukaryotes. *Adv. Exp. Med. Biol.* **702,** 122–131
55. Kuehner, J. N., Pearson, E. L., and Moore, C. (2011) Unraveling the means

to an end. RNA polymerase II transcription termination. *Nat. Rev. Mol. Cell Biol.* **12,** 283–294
56. Steinmetz, E. J., Warren, C. L., Kuehner, J. N., Panbehi, B., Ansari, A. Z., and Brow, D. A. (2006) Genome-wide distribution of yeast RNA polymerase II and its control by Sen1 helicase. *Mol. Cell* **24,** 735–746
57. Steinmetz, E. J., Conrad, N. K., Brow, D. A., and Corden, J. L. (2001) RNA-binding protein Nrd1 directs poly(A)-independent 3′ end formation of RNA polymerase II transcripts. *Nature* **413,** 327–331
58. O'Sullivan, J. M., Tan-Wong, S. M., Morillon, A., Lee, B., Coles, J., Mellor, J., and Proudfoot, N. J. (2004) Gene loops juxtapose promoters and terminators in yeast. *Nat. Genet.* **36,** 1014–1018
59. Lainé, J. P., Singh, B. N., Krishnamurthy, S., and Hampsey, M. (2009) A physiological role for gene loops in yeast. *Genes Dev.* **23,** 2604–2609
60. Ansari, A., and Hampsey, M. (2005) A role for the CPF 3′ end processing machinery in RNAP II-dependent gene looping. *Genes Dev.* **19,** 2969–2978
61. Brickner, J. H. (2009) Transcriptional memory at the nuclear periphery. *Curr. Opin. Cell Biol.* **21,** 127–133
62. Kim, H. D., Choe, J., and Seo, Y. S. (1999) The *sen1*$^+$ gene of *Schizosaccharomyces pombe*, a homologue of budding yeast SEN1, encodes an RNA and DNA helicase. *Biochemistry* **38,** 14697–14710
63. Mischo, H. E., Gómez-González, B., Grzechnik, P., Rondón, A. G., Wei, W., Steinmetz, L., Aguilera, A., and Proudfoot, N. J. (2011) Yeast Sen1 helicase protects the genome from transcription-associated instability. *Mol. Cell* **41,** 21–32
64. Skourti-Stathaki, K., Proudfoot, N. J., and Gromak, N. (2011) Human senataxin resolves RNA/DNA hybrids formed at transcriptional pause sites to promote Xrn2-dependent termination. *Mol. Cell* **42,** 794–805
65. Aguilera, A., and García-Muse, T. (2012) R loops. From transcription by-products to threats to genome stability. *Mol. Cell* **46,** 115–124
66. Gómez-González, B., García-Rubio, M., Bermejo, R., Gaillard, H., Shirahige, K., Marín, A., Foiani, M., and Aguilera, A. (2011) Genome-wide function of THO/TREX in active genes prevents R-loop-dependent replication obstacles. *EMBO J.* **30,** 3106–3119
67. Houseley, J., Kotovic, K., El Hage, A., and Tollervey, D. (2007) Trf4 targets ncRNAs from telomeric and rDNA spacer regions and functions in rDNA copy number control. *EMBO J.* **26,** 4996–5006
68. Yadon, A. N., Van de Mark, D., Basom, R., Delrow, J., Whitehouse, I., and Tsukiyama, T. (2010) Chromatin remodeling around nucleosome-free regions leads to repression of noncoding RNA transcription. *Mol. Cell. Biol.* **30,** 5110–5122
69. Kar, A., Fushimi, K., Zhou, X., Ray, P., Shi, C., Chen, X., Liu, Z., Chen, S., and Wu, J. Y. (2011) RNA helicase p68 (DDX5) regulates tau exon 10 splicing by modulating a stem-loop structure at the 5′ splice site. *Mol. Cell. Biol.* **31,** 1812–1821
70. Suzuki, H. I., Yamagata, K., Sugimoto, K., Iwamoto, T., Kato, S., and Miyazono, K. (2009) Modulation of microRNA processing by p53. *Nature* **460,** 529–533
71. Cohen, A. A., Geva-Zatorsky, N., Eden, E., Frenkel-Morgenstern, M., Issaeva, I., Sigal, A., Milo, R., Cohen-Saidon, C., Liron, Y., Kam, Z., Cohen, L., Danon, T., Perzov, N., and Alon, U. (2008) Dynamic proteomics of individual cancer cells in response to a drug. *Science* **322,** 1511–1516
72. Fuller-Pace, F. V., and Moore, H. C. (2011) RNA helicases p68 and p72. Multifunctional proteins with important implications for cancer development. *Future Oncol.* **7,** 239–251
73. Zuker, M. (2003) Mfold web server for nucleic acid folding and hybridization prediction. *Nucleic Acids Res.* **31,** 3406–3415
74. Tajima, M., Nogi, Y., and Fukasawa, T. (1986) Duplicate upstream activating sequences in the promoter region of the *Saccharomyces cerevisiae GAL7* gene. *Mol. Cell. Biol.* **6,** 246–256